

# **Impact of leachate filtration on slope failure potential of landfill side walls**

Damjan Ivetić and Nenad Jaćimović

Faculty of Civil Engineering, University of Belgrade, Belgrade, 11000, Serbia

## **Corresponding author:**

D. Ivetić, Faculty of Civil Engineering, University of Belgrade, Belgrade, 11000, Serbia

E-mail: [divetic@hikom.grf.bg.ac.rs](mailto:divetic@hikom.grf.bg.ac.rs)

## **Abstract**

The most common method for organized solid waste disposal, in middle and low income countries, is certainly the use of landfills. Although design of those structures has been improved significantly during the last decades, there are still potential hazards that require attention. In this paper, one of the many possible hazardous scenarios has been investigated. In the event of heavy precipitation leachate head is rising in the body of active landfill presuming there is no daily cover above the body. Due to leachate drainage malfunction, leachate head can rise above the design criteria value. With the landfill sidewall geomembrane previously damaged, or poorly built, gravity will drive the leachate through porous side walls of landfill. Gravity-driven groundwater flow will influence the distribution of effective stress in the body of a side wall. Effective stress, in turn, influences the potential for shear slope failure which can be quantified using the Coulomb failure potential. For evaluation of the effects of leachate filtration, we formulate a two-dimensional, steady state, poroelastic model. Steady state filtration model is formulated for unsaturated/saturated porous media. For the illustration, leachate flow field, total body force field and effective stress field are calculated in a landfill side wall. Based on this results Coulomb failure potential field is calculated for the body of a side wall. In most parts leachate flow significantly increases the value of the failure potential, while shifting the locus of greatest values towards the toe of the outer slope of a side wall.

Keywords: failure potential, filtration, landfills, leachate

## **1. INTRODUCTION**

Organized solid waste disposal in middle and low income countries depends mostly on the use of sanitary landfills. Landfilling is often the choice method for waste

management owing to its low costs, its ready availability and its applicability to a wide range of wastes (Williams, 2005). High income societies are exploiting some newer technologies, for example solid waste incineration, separation and recycling etc. Recent studies showed that for medium sized city of Novi Sad in Serbia, although external financial assistance is necessary, investments like mass burn incineration facility can be positive (Mikic and Naunovic, 2013). As it is well known in scientific society, risks for public health originate from the way the waste is (or is not) handled, stored, collected and disposed. Statistics say that in poorer parts of world estimated 30 to 50% of solid wastes produced in urban areas are left uncollected, constantly posing threat for public health (Rushbrook and Pugh, 1999). Small cities usually cannot afford to operate a sanitary landfill, but sustainable solution has been recently proposed based on the experience from Villanueva, Honduras (Oakley and Jimenez, 2012).

Having this in mind it is reasonable and well justified to investigate the operating conditions and investigate the potential hazards of use of landfills. Thanks to the rising awareness on the issue of solid waste disposal and effort of the scientific community, different aspects of sanitary landfill design and exploitation have been examined and improved in past (Schiappacasse et al, 2010). Still there are a number of potential hazards that require attention in landfill design.

This paper is addressing the issue of leachate filtration through porous walls of landfills. Leachate is generated from the waste itself and by precipitation event if the daily cover over the active field is not applied. Design criteria for the drainage system will impose maximal head value for leachate generated in the body of a landfill. Usually leachate should be managed by the drainage system constructed in the operating landfill, whose task is to collect and drive leachate safely to the sewer system. It is possible, especially in the case of poor maintenance, that the drainage will be out of order or not working properly due to the clogging (Rowe and Yu, 2012). Maintenance crew will probably not recognize the problem until the event of heavy precipitation. When heavy rain occurs with no daily cover, leachate head will raise above the design criteria value.

Landfill walls are usually made of local materials (Pitchel, 2005), making the porous medium through which a fluid can flow. Inner slopes of walls are covered with the geomembrane, whose task is to prevent leachate filtration through a wall of sanitary landfill. If the geomembrane is previously damaged or poorly built, event of heavy precipitation will cause this membrane to deteriorate, and leave the inner slope vulnerable to leachate. Gravity will drive leachate from the landfill body through the landfill wall. Fluid filtration through porous media creates body forces which will now act inside the landfill sidewall. Body forces formed by this way are seepage and buoyancy force. Goal of this analysis is to investigate the effects of this body forces on the potential for shear slope failure of the landfill sidewalls.

## 2. MODEL DESCRIPTION

In this part, basic equations governing the issue of a steady state, 2D filtration and poroelastic analysis are presented. Saturated/unsaturated flow through porous media was described using the van Genuchten soil characteristic curve (van Genuchten, 1980) and Mualem's model for reduced soil conductivity (Mualem, 1976). Description is brief, due to the fact that emphasis of the paper is not on the mathematical model.

### 2.1. Flow through the porous media

For representation of steady state fluid flow through porous media, Darcy's law (Charbeneau, 2000) is employed. Itself it summarizes majority of physics of groundwater flow (Eq. 1), by stating that the velocity vector is dictated by potential gradient  $\frac{dh}{dl}$  and hydraulic conductivity  $K$  :

$$q = \frac{Q}{A} = -K \frac{dh}{dl} \quad (1)$$

where  $Q$  is the flow rate, while  $q$  is Darcian velocity or flow rate per unit area of porous medium. Fluid potential at a given point is the energy required to transport a unit mass of water from a standard reference state to that point. Differences in potential will make fluid flow, from higher potential to lower potential (Wang and Anderson, 1982). Combining Darcy's law with the continuity equation, for a 2D steady state conditions, partial differential Laplace's equation for anisotropic and heterogenic domain can be derived:

$$\frac{\partial}{\partial x} \left( -K_x \frac{\partial h}{\partial x} \right) + \frac{\partial}{\partial y} \left( -K_y \frac{\partial h}{\partial y} \right) = 0 \quad (2)$$

If the flow domain is not completely saturated, unsaturated flow conditions occur. In saturated region pressure is positive whilst in unsaturated, or vadose zone, it is negative and usually is called capillary pressure (Charbeneau, 2000). Unsaturated flow theory has been intensively investigated in the 70's and 80's deriving several analytical models for definition of soil water characteristic curve (van Genuchten, 1980). The soil water characteristic curve provides the relationship between the capillary pressure ( $\Psi$ ) and water content for a particular soil ( $\theta_w$ ). Reduction of water content influences hydraulic conductivity of the porous media, which can be described with Mualem's model for

relative permeability. In this study, Van Genuchten's definition of soil water characteristic curve is utilized, coupled with relative permeability model.

Governing relationship of the van Genuchten's model is:

$$\theta = \frac{\theta_w - \theta_r}{\theta_s - \theta_r} = \left( \frac{1}{1 + (\alpha\Psi)^N} \right)^M \quad (3)$$

for  $\Psi \geq 0$ , where  $\theta$  is reduced saturation,  $\theta_r$  irreducible saturation,  $\theta_s$  saturated water content while  $\alpha$ ,  $N$  and  $M$  are parameters of van Genuchten model. Soil characteristic curve resulting from this model is continuous throughout the  $\Psi \geq 0$  making it preferable for numerical modelling. With Mualem's relative conductivity model, parameters  $N$  and  $M$  are related through  $M = 1 - 1/N$  or  $N = 1/(1 - M)$ . Hydraulic conductivity in unsaturated porous media is obtained from two parameters, hydraulic conductivity at saturation  $K_{ws}$  or just  $K$ , and the relative permeability  $k_{rw}$  through following equation:

$$K_w(\theta_w) = k_{rw}(\theta_w)K \quad (4)$$

To obtain a value for  $k_{rw}$  Mualem's model is implemented, which uses the same parameters as in equation (3):

$$k_{rw} = \sqrt{\theta} \left( 1 - [1 - \theta^{1/M}]^M \right)^2 \quad (5)$$

By applying described closure relations, the solution of Laplace's equation (2) provides the unknown hydraulic head and consequently gradients and seepage forces in the flow domain.

## 2.2. Elastic displacements analysis

Formulation presented in this paper is similar to the one presented by Iverson and Reid (1992), restricted to the plane strain and with the clear highlight on the role of gravitational potential and body forces.

Fundamental equations for this analysis are those that define infinitesimal strains in the solid porous medium using the displacement gradients:

$$\begin{aligned}
\varepsilon_{xx} &= \frac{\partial u_x}{\partial x} \\
\varepsilon_{yy} &= \frac{\partial u_y}{\partial y} \\
\varepsilon_{xy} &= \frac{1}{2} \left( \frac{\partial u_x}{\partial y} + \frac{\partial u_y}{\partial x} \right)
\end{aligned} \tag{6}$$

Where  $u_x$  and  $u_y$  are the components of solid displacement in the  $x$  and  $y$  directions,  $\varepsilon_{xx}$  and  $\varepsilon_{yy}$  are normal strains in these directions while  $\varepsilon_{xy}$  is shear strain in the  $x$  direction on planes normal to  $y$ . Strain tensor is symmetric so shear strains on orthogonal planes are equal:  $\varepsilon_{xy} = \varepsilon_{yx}$ . Previous equations are valid regardless of stress definitions and material behaviour and are important since boundary conditions and governing equations are specified in terms of the solid displacement (Iverson and Reid, 1992).

Next, equations for stress equilibrium in a porous media with steady fluid flow, need to be defined. Since presence of water in porous media define effective stresses as a sole cause of elastic strains, emphasis is made on the effective stress equilibrium. Terzaghi (1923) developed the effective stress concept in which a general definition of effective stress is:

$$\sigma'_{ij} = \sigma_{ij} + \alpha p \delta_{ij} \tag{7}$$

where  $\sigma_{ij}$  is the total stress,  $p$  is the pore water pressure and  $\delta_{ij}$  is the Kronecker delta operator. The value of  $\alpha$  can be defined on different ways, but here is adopted to be simply  $\alpha = 1$ , which corresponds to the steady state fluid flow.

If  $y$  coordinate is directed vertically upwards, effective stress equilibrium equations in both Cartesian coordinates can be defined as:

$$\begin{aligned}
\frac{\partial \sigma'_{xx}}{\partial x} + \frac{\partial \sigma'_{yx}}{\partial y} &= \alpha \rho_w g \frac{\partial h}{\partial x} \\
\frac{\partial \sigma'_{yy}}{\partial y} + \frac{\partial \sigma'_{yx}}{\partial x} &= (\rho_t - \alpha \rho_w) g + \alpha \rho_w g \frac{\partial h}{\partial y}
\end{aligned} \tag{8}$$

All body forces of interest are here presented, with terms containing the head gradient representing the seepage forces acting in  $x$  and  $y$  direction and submerged-unit-weight

term  $(\rho_t - \alpha\rho_w)g$  represents the hydrostatic buoyancy effect. To determine the three unknown components of stress in the eq. (8), constitutive equations are employed that relate stress to strains in the solid porous medium. Equations for total stresses reduce to standard Hooke's law constitutive equations for effective stresses of a form:

$$\begin{aligned}\varepsilon_{xx} &= \frac{1}{E} \left[ (1-\nu^2)\sigma'_{xx} - \nu(1+\nu)\sigma'_{yy} \right] \\ \varepsilon_{yy} &= \frac{1}{E} \left[ (1-\nu^2)\sigma'_{yy} - \nu(1+\nu)\sigma'_{xx} \right] \\ \varepsilon_{yx} &= \frac{1+\nu}{E} \sigma'_{yx}\end{aligned}\tag{9}$$

Here  $E$  is the Young's modulus and  $\nu$  is the drained Poisson's ratio of the solid porous medium. Strictly speaking different formulation was used here for effective stresses then presented in eq. (7), in order to derive appropriate constitutive equations. But even in this different approach if we adopt that constituent particles composing the solid porous medium are much less compressible than is the porous medium as a whole, effective stress definition is the same as stated earlier.

In order to mathematically complete the set of equations governing the effective stress problem, effective stress compatibility equation is derived from constitutive, stress equilibrium and strain compatibility equations. Last one is omitted in this paper since it can be easily obtained from eq (6). Compatibility equation in terms of effective stresses and hydraulic gradients, for anisotropic and heterogenic medium has the following form:

$$\left( \frac{\partial^2}{\partial x^2} + \frac{\partial^2}{\partial y^2} \right) (\sigma'_{xx} + \sigma'_{yy}) = \frac{1}{1-\nu} \left[ \rho_w g \left( \frac{\partial^2 h}{\partial x^2} + \frac{\partial^2 h}{\partial y^2} \right) + g \frac{\partial \rho_t}{\partial y} \right]\tag{10}$$

For fluid flow through homogenous and isotropic medium and for uniform bulk density of porous medium right hand side is equal to zero.

Mathematical model needs to be recast in terms of displacements instead of stresses, since the boundary conditions are stated as solid displacements. Combining equations (6), (8) and (9) whilst employing some algebraic manipulation, can result in two equations for the components of displacement  $u_x$  and  $u_y$ :

$$\frac{E}{2(1+\nu)} \nabla^2 u_x + \left[ \frac{\nu E}{(1-2\nu)(1+\nu)} + \frac{E}{2(1+\nu)} \right] \cdot \left( \frac{\partial^2 u_x}{\partial x^2} + \frac{\partial^2 u_y}{\partial y \partial x} \right) = \rho_w g \frac{\partial h}{\partial x}$$

$$\frac{E}{2(1+\nu)} \nabla^2 u_y + \left[ \frac{\nu E}{(1-2\nu)(1+\nu)} + \frac{E}{2(1+\nu)} \right] \cdot \left( \frac{\partial^2 u_y}{\partial y^2} + \frac{\partial^2 u_x}{\partial x \partial y} \right) = (\rho_t - \rho_w) g + \rho_w g \frac{\partial h}{\partial y}$$
(11)

It can be seen that in the equations above as well as in those governing groundwater flow and effective stress fields, the consequence of uniform pore pressure change is zero, since such change doesn't influence the value of  $\partial h/\partial x$  and  $\partial h/\partial y$  (Iverson and Reid, 1992). This implies that equations (11) can be applied, without modification to materials with no groundwater flow, or, if  $\rho_w$  is set equal to 0, to materials with no pore water.

### 2.3. Boundary conditions

Set of boundary conditions must be defined for the equations (2) and (11). Idea is to reflect characteristics of the leachate filtration through landfill wall. Boundary conditions for this case must incorporate following features: a) that there is no influence of the bottom boundary condition on flow and stresses near surface b) that solid waste from the landfill body abut on the inner side of the wall c) that there is no force acting on the rest of the wall surface. For the definition of conditions, reference to figure 1 is made, where a solution domain is presented.

Equation (2) requires boundary conditions from both left and right side of a landfill wall in order to determine a head distribution and fluid's phreatic surface. Boundary conditions are defined in terms of head values at the slopes of the landfill wall.

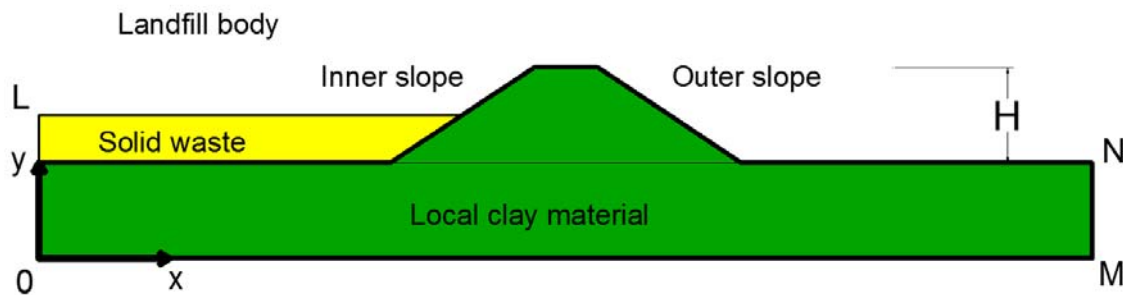


Figure 1. Geometry of the solution domain for the landfill example problem

At beginning only the inner slope can get an exact boundary condition since it is a side where we can define a head of leachate in a body of landfill:

$$h(x_{LB}, y_{LB}) = h_L \quad (12a)$$

where  $(x_{LB}, y_{LB})$ , corresponds to the left or inner slope of wall. Since at start it is unknown where the free surface of leachate will intersect the outer slope, it is most convenient to start from:

$$h(x_{RB}, 0) = 0 \quad (12b)$$

where  $(x_{RB}, 0)$ , corresponds to the beginning of the slope on the outer side. Computation of outer boundary condition will need several iterations in which this boundary condition is updated for every node placed on the outer wall surface in which calculated value for  $h$  exceeds the height of that node  $y$ . These nodes will have a boundary head value equal to the  $y$ :

$$h(x_{RB}, y_{RB}) = y_{RB} \quad (13)$$

To conclude, a set of no flow boundary conditions needs to be defined for both lateral and bottom margins of the domain. This is appropriate since the margins are far enough from the wall itself and should not affect the groundwater flow. This can be presented as:

$$\frac{\partial h}{\partial x}(0, y) = 0 \quad (14a)$$

$$\frac{\partial h}{\partial x}(x_M, y) = 0 \quad (14b)$$

$$\frac{\partial h}{\partial y}(x, 0) = 0 \quad (14c)$$

In order to round up this problem, boundary conditions for Eq. (11) need to be addressed. Solid displacements are defined for the lateral and bottom margin of the



domain. Since behind lateral margins of the domain, there is no major change in topography, horizontal displacements on these lateral margins are restricted. It can be stated mathematically as:

$$u_x(0, y) = 0 \quad (15a)$$

$$u_x(x_M, y) = 0 \quad (15b)$$

Finite bottom boundary depth feature implies that bottom margin of the domain will have both horizontal and vertical displacements equal to zero:

$$u_x(x, 0) = 0 \quad (15c)$$

$$u_y(x, 0) = 0 \quad (15d)$$

Finally effects of the solid waste abutting on the inner side of the landfill wall need to be discussed. This boundary condition was presented through expended finite element mesh, which will represent the solid waste itself. Actual solid waste represented in the figure 1 is modelled as part of the finite element mesh with its unit-weight body forces acting in the finite elements. This way, effects of the weight body forces originating from the solid waste mass are incorporated in the boundary problem. It is questionable how large this solid waste pile inside the landfill cell should be for this analysis, since its actual volume will determine the value of forces acting on the outer slope of the landfill wall. For this model, height of the solid waste pile was half of the landfill wall height which would correspond to active landfill cell that is neither empty nor full.

#### **2.4. Coulomb failure potential**

In order to quantify the effects off the leachate filtration through landfill wall, Coulomb potential for shear failure is used. To compute this value, principal stresses need to be obtained first. Plane strain analysis implies that only two principal stresses ( $\sigma_1$  and  $\sigma_3$ ) can be obtained which represent maximum and minimum normal stresses acting in plane where the shear stress is zero. Relationships for their computation can be found in literature (Verujit, 2001).

Coulomb failure potential is derived from the Coulomb failure rule, which can be written in the form:

$$\frac{\sigma_1 - \sigma_3}{\sigma_1 + \sigma_3} = \frac{|\tau'_{\max}|}{-\sigma'_m} = \sin \phi = \Phi \quad (16)$$

where  $\tau_{max}$  is the maximum shear stress,  $\sigma'_m$  is the mean normal stress, and  $\phi$  is the angle of internal friction. Calculation of the orientation and magnitude of the stresses acting on a failure plane requires knowledge of the angle of internal friction. Instead of using the laboratory or field tests to determine  $\phi$ , the stress ratio presented in eq. 16 is used as a dimensionless measure of shear failure potential. Coulomb failure potential is independent of the material strength and has a theoretical minimum of zero and maximum of one. If a computed value is outside this margins, it means that one of the principal stresses is tensile. Cohesionless materials cannot withstand tension so in this case, the value of  $\Phi$  is unimportant.

### 3. NUMERICAL SOLUTION

Problem defined by (2), (11), (12a), (12b), (13), (14a)-(14c), and (15a)-(15d) was solved using two finite element models. First one is a groundwater flow model, designed for both saturated and unsaturated conditions. This model is employed only in the case where actual geomembrane on the landfill wall was damaged, so it allows a leachate filtration through sidewall. Second finite element model is used for the elastic displacements. Both models use bilinear, four-node, quadrilateral and continuum elements.

For the first scenario, in which geomembrane is still intact and there is no leachate seeping through the landfill wall, first computation step is to obtain the nodal displacements. Next, strains are calculated and finally through Hooke's law effective stress distribution is obtained. In the second scenario, there is a leachate flow through a landfill flow which influences the body forces distribution. This means that first groundwater flow model must be employed to determine head distribution and leachate free surface. It is important to state that only bellow leachate phreatic line will the body forces originating from the leachate flow, be introduced. Using the results of the groundwater model computations as the input for the elastic displacement model, new nodal displacements are calculated. Again through average strains, effective stress distribution is determined using the appropriate model.

Finite element mesh grid used for the analysis presented in this paper is the same for both finite element models. Mesh is made of 1242 quadrilateral elements. Using the same mesh means that there is no post-processing needed in order to use the results of the groundwater flow model inside the elastic displacement model.

#### 4. RESULTS AND DISCUSSION

In this section numerical results of the leachate filtration and elastic displacement analysis are presented for the landfill wall composed of homogenous clay material. This analysis illustrate influence of the leachate filtration on the effective stress distribution and ultimately on the potential for shear failure. As stated earlier both local clay material, that composes landfill wall and surroundings, and solid waste were modelled. Filtration and elastic displacement results regarding solid waste are not of interest and will be omitted. Parameters used for these materials in both models are presented in table 1.

**Table 1. Parameters for local clay material and solid waste**

		Parameters for elastic displacement analysis					
Material	Dry density	Saturated density	Poisson's ratio	Young's modulus			
	$\rho_{td}$	$\rho_{ts}$	$\nu$	$E$			
	[kg/m <sup>3</sup> ]	[kg/m <sup>3</sup> ]	[/]	[MPa]			
Local clay	1600	2000	0.3	50			
Solid waste	770	1000	0.33	1			
		Parameters for groundwater flow analysis					
Material	Hydraulic conductivity x	Hydraulic conductivity y	Residual w. content	Saturated w. content	Model par.	Model par.	
	$K_x$	$K_y$	$\theta_r$	$\theta_w$	$\alpha$	$n$	
	[m/s]	[m/s]	[/]	[/]	[/]	[/]	
Local clay	0.0000001	0.00000001	0.19	0.4	0.8	1.3	
Solid waste*	0.0001	0.00001	0	0.23	2	2.9	

\* Solid waste parameters for the groundwater analysis are most similar to the ones used for gravel type materials

Numerical results are reduced by nondimensionalization of the variables, as presented in table 2. It should be noted that all lengths are scaled by  $H$ , wall height, while body forces are scaled by  $\rho_w g$ .

**Table 2. Nondimensionalization of variables in the model computations**

Quantity	Dimensions	Nondimensional quantity
x, y, h (length)	L	x/H, y/H, h/H
$\rho_t$ (bulk density)	$ML^{-3}$	$\rho_t/\rho_w$
F (body forces)	$ML^{-2}T^{-2}$	$F/\rho_w g$
$\sigma'_{ij}, H_{mat}$ (effective stress, matric potential)	$ML^{-1}T^{-2}$	$\sigma'_{ij}/\rho_w g H, H_{mat}/\rho_w g H$

Three different scenarios (Fig.2) were examined in which different values for the leachate head are used:

- a)  $h = \frac{1}{4} H$
- b)  $h = \frac{1}{2} H$
- c)  $h = \frac{3}{4} H$

Third scenario is unlikely to occur unless landfill side walls are small in height, but was tested nevertheless in order to try to invoke near maximum values for  $\Phi$ . Leachate filtration scenarios were compared to normal operating conditions inside landfill body. Due to operating drainage system and geomembrane intact, leachate head build-up doesn't occurs so the landfill wall is essentially dry. Body forces distribution in dry conditions is uniform, but in the case of the leachate filtration, due to the contribution from the seepage forces, it will become irregular. First body force distribution is presented for the scenario c) in figure 3. On the same figure phreatic line of leachate is presented in order to distinguish the saturated and unsaturated zones. Similar results were obtained for other two scenarios.

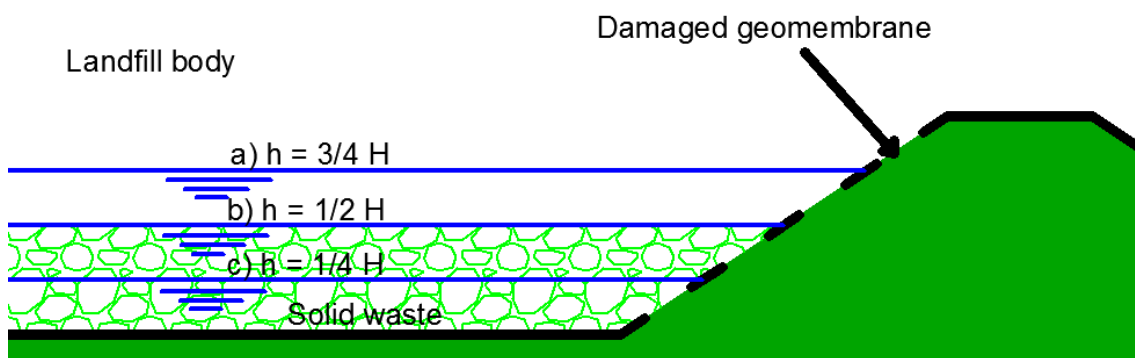


**Figure 2. Three scenarios of leachate head build-up**

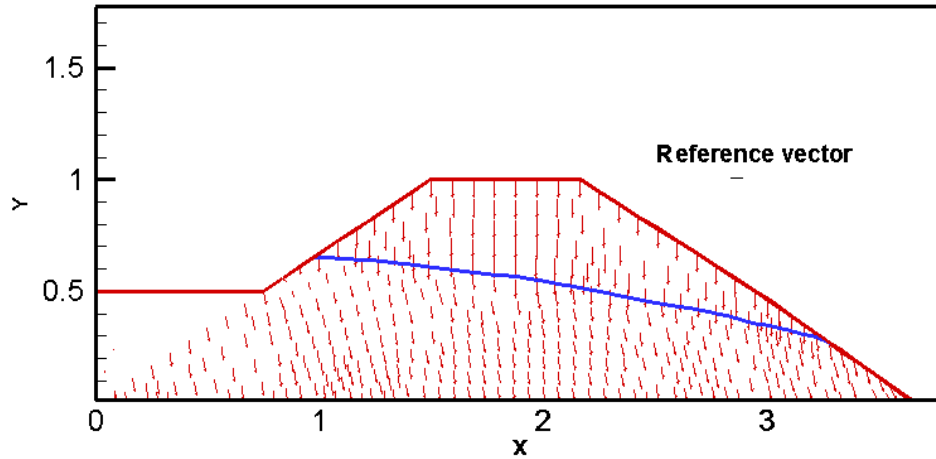


**Figure 3. Total body force vector distribution for scenario c)**

Results illustration is concluded with  $\Phi$  distribution for the normal operating conditions presented in figure 4, followed by the ones for the scenarios a), b) and c) in figures 5, 6 and 7 respectively. Coulomb failure distributions are presented for the landfill wall outer slope, where highest influence from the leachate filtration was noticed.

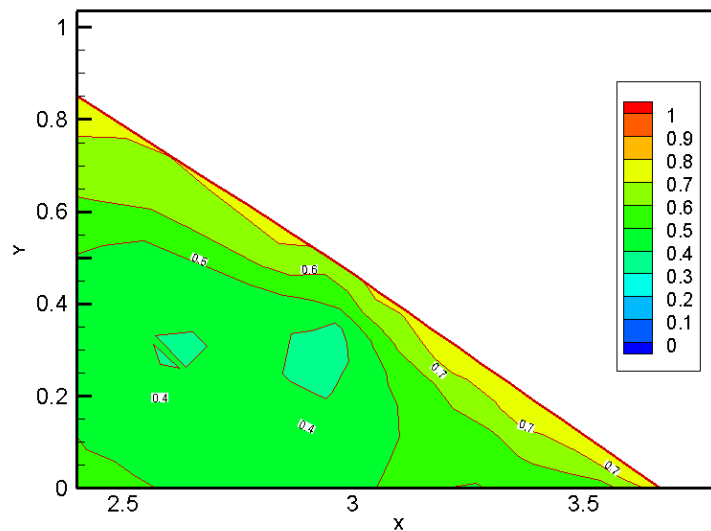


**Figure 4. Coulomb failure potential distribution on the outer slope of the wall for normal operating conditions**

On figures 5, 6 and 7 along with the Coulomb failure potential, leachate free surface lines are presented.

Leachate filtration induces two additional body forces compared to the normal operating conditions, buoyancy force acting vertically upwards and seepage force acting in the direction of the head gradient. These forces act only in the saturated part of the wall body. Buoyancy force actually reduces weight of the soil in the saturated region according to Archimedes' law.

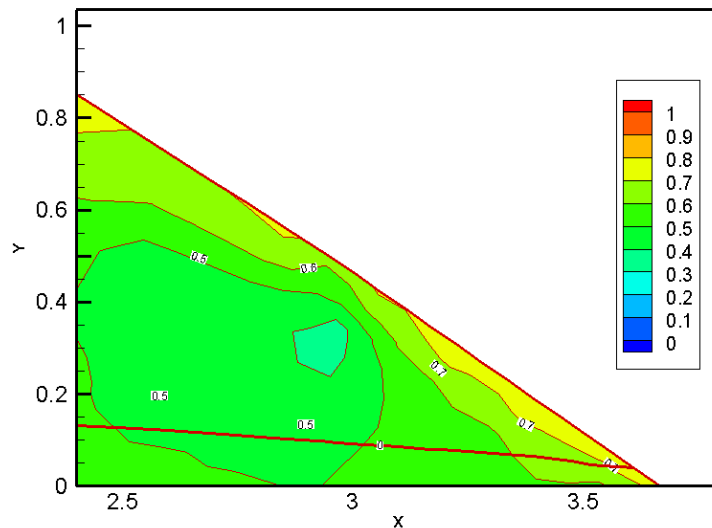


**Figure 5. Coulomb failure potential distribution and leachate phreatic line, near the toe of the outer slope of the wall for the scenario a)**

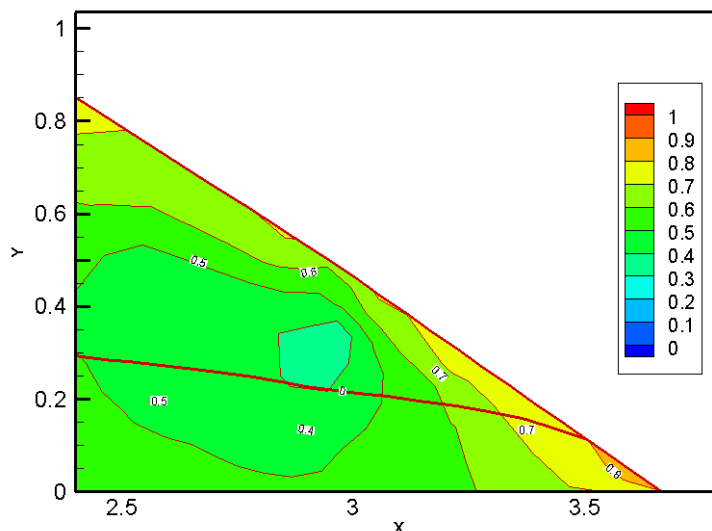


**Figure 6. Coulomb failure potential distribution and leachate phreatic line, near the toe of the outer slope of the wall for the scenario b)**

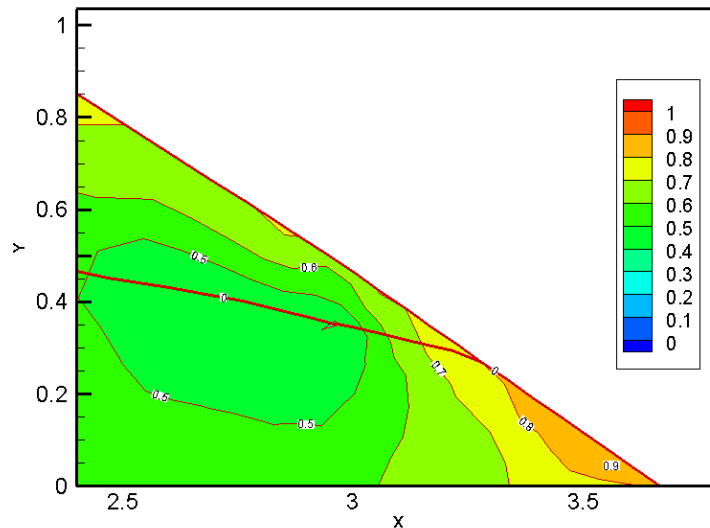


**Figure 7. Coulomb failure potential distribution and leachate phreatic line, near the toe of the outer slope of the wall for the scenario c)**

For the scenario a) where the solid waste inside the landfill body still is not completely submerged, weight body forces from the waste itself actually contribute to the slope stability. For the scenarios b) and c) weight and buoyancy forces cancel each other out. It can be observed from the figures 3 that below phreatic line seepage force induces the change in the total body vector orientation, rotating it in  $x$  direction. Most significant rotation of all three cases is illustrated, which is expected since largest head gradients in  $x$  direction are found in this case.

Comparing figures 4, 5, 6 and 7 implies that the increase of the value of Coulomb failure potential is most significant at the toe of the outer slope. Leachate filtrating through the porous body of the wall, exits the body at the slope toe. Exfiltration surface depends on the value of the leachate head inside the landfill body, increasing along with the head. Highest increase of the Coulomb failure potential, compared to the “dry” conditions, is in the region of exfiltration. Due to the fact that head gradients near this region are almost perpendicular to the slope surface, seepage forces directed outwards, induce the significant increase in the shear stress. Scenario a) shows negligible influence of the leachate filtration on the shear stress distribution as the values do not differ much from the normal operating conditions. Already in scenario b) increase to the maximum value of 0.85 for Coulomb failure potential is observed near the slope toe. In the last examined scenario exfiltration region is more than twice the size of the previous case, with Coulomb failure potential reaching the maximum value of 0.93.

## 5. CONCLUSIONS

A numerical model for simulation of fluid flow in saturated and unsaturated porous media coupled with elastic displacement analysis was developed. In this study, model is applied for simulation of a leachate filtration through homogeneous and anisotropic sidewall of a sanitary landfill in order to investigate effects of leachate flow on effective stresses in the porous medium and ultimately on shear failure potential.

Assuming the porous media as elastic, it was found that water flow significantly influence the failure potential, which was quantified by calculation of the Coulomb failure potential. The most significant effects are observed at the outer slope toe, where, for applied leachate filtration scenarios, the maximum increase of Coulomb failure potential was about 30%.

Since the generated leachate inside the sanitary landfill usually contains a variety of contaminants, uncontrolled exfiltration from the landfill can have a negative impact on the environment. Intention is to extend developed model by including contaminant in order to analyse this effects.

## Acknowledgements

The authors wish to express gratitude to the Ministry of Science, Education and Technological Development of the Republic of Serbia for the support in project TR37010 entitled "Rain water drainage systems as part of the urban and transport infrastructure" whose part was the research presented in this paper.

## References

- 1) Charbeneau, R., (2000). Groundwater Hydraulics and Pollutant Transport, Prentice-Hall Inc., New Jersey, 589 p.
- 2) Iverson, R., Reid, M., (1992). Gravity-Driven Groundwater Flow and Slope Failure Potential 1. Elastic Effective-Stress Model, Water Resources Research, vol. 28, No. 3, p. 925-938.
- 3) Mikić, M., Naunović Z., (2013). A sustainability analysis of an incineration project in Serbia. Waste Management & Research, Vol. 31, p. 1102-1109.
- 4) Mualem, Y. (1976). A new model for predicting the hydraulic conductivity of unsaturated porous media. Water Resources Research, Vol.12. p. 593-622.
- 5) Oakley, S.M., Jimenez, R. (2012). Sustainable sanitary landfills for neglected small cities in developing countries: The semi-mechanized trench method from Villanueva, Honduras. Waste Management, Vol.32, p. 2535-2551.
- 6) Pitchel, J., (2005). WASTE MANAGEMENT PRACTICES: Municipal, Hazardous and Industrial, Taylor & Francis Group, Boca Raton, 690 p.
- 7) Rowe, R.K., Yu, Y. (2012). Clogging of finger drain systems in MSW landfills. Waste Management, Vol.32, p. 2342-2352.



- 8) Rushbrook, P., Pugh, M. (1999). Solid Waste Landfills in Middle- and Lower- Income Countries, The International Bank for Reconstruction and Development/THE WORLD BANK, Washington D.C. 248 p.
- 9) Schiappacasse, M.C., Palma J., Poirrier, P., Ruiz-Filippi, G., Chamy, R., (2010). Improved sanitary landfill design using recirculation of anaerobically treated leachates: generation of advanced design criteria. *Electronic Journal of Biotechnology*, Vol. 13.
- 10) Terzaghi, K. (1923). Die Berechnung der Durchlässigkeit des Tones aus dem Verlauf der hydrodynamischen Spannungsercheinungen. *Akad. Wiss. Wien Math. Naturwiss, Sitzungsber. Abt. 2A*, 132. p. 105-124.
- 11) Van Genuchten, M.T, (1980). A Closed-Form Equation for Predicting the Hydraulic Conductivity of Unsaturated Soil, *Soil Sci. Soc. Am. J.*, Vol. 44, p. 892-898.
- 12) Verujit, A. (2001). *Soil Mechanics*. Screenbook version of the book, Delft University of Technology.
- 13) Wang, F.H., Anderson, P.M. (1982). *Introduction to groundwater modeling: Finite Difference and Finite Element Methods*. Academic press, San Diego, USA.
- 14) Williams, P.T. (2005). *Waste Treatment and Disposal*. 2nd ed. Chichester: John Wiley.